

Mitochondrial redox signalling by p66Shc mediates ALS-like disease through Rac1 inactivation

Maria Grazia Pesaresi^{1,5}, Ilaria Amori¹, Carlotta Giorgi², Alberto Ferri³, Paolo Fiorenzo¹, Francesca Gabanella³, Anna Maria Salvatore³, Marco Giorgio⁴, Pier Giuseppe Pelicci⁴, Paolo Pinton², Maria Teresa Carri^{1,5,†} and Mauro Cozzolino^{1,*,†}

¹Laboratory of Neurochemistry, Fondazione S. Lucia IRCCS, Rome, Italy, ²Section of General Pathology, Department of Experimental and Diagnostic Medicine, Interdisciplinary Center for the Study of Inflammation (ICSI) and LTTA Center, University of Ferrara, Ferrara, Italy, ³Institute of Cell Biology and Neurobiology, Rome, Italy, ⁴IFOM-IEO Campus, Milan, Italy and ⁵Department of Biology, University of Rome Tor Vergata, Via della Ricerca Scientifica, Rome, Italy

Received June 15, 2011; Revised and Accepted August 4, 2011

Increased oxidative stress and mitochondrial damage are among the mechanisms whereby mutant SOD1 (mutSOD1) associated with familial forms of amyotrophic lateral sclerosis (ALS) induces motoneuronal death. The 66 kDa isoform of the growth factor adapter Shc (p66Shc) is known to be central in the control of mitochondria-dependent oxidative balance. Here we report that expression of mutSOD1s induces the activation of p66Shc in neuronal cells and that the overexpression of inactive p66Shc mutants protects cells from mutSOD1-induced mitochondrial damage. Most importantly, deletion of p66Shc ameliorates mitochondrial function, delays onset, improves motor performance and prolongs survival in transgenic mice modelling ALS. We also show that p66Shc activation by mutSOD1 causes a strong decrease in the activity of the small GTPase Rac1 through a redox-sensitive regulation. Our results provide new insight into the potential mechanisms of mutSOD1-mediated mitochondrial dysfunction.

INTRODUCTION

Damage to mitochondria is emerging as a central feature that contributes to the degeneration of motor neurons in amyotrophic lateral sclerosis (ALS). Recent evidence indicates that mitochondria are one of the primary location of damage inside motor neurons (1), but also astrocytes and muscle cells, which both have been involved in the disease, show deficits in mitochondrial metabolism (2–4). Dysfunction of mitochondria is observed early in patients (and in experimental models for ALS) and causes the death of neurons, which underlies onset of paralysis and death of patients. A large body of studies in cells and mice overexpressing mutSOD1s, which model many characteristics of the disease, have addressed different aspects of mitochondrial dysfunction occurring in ALS, ranging from altered morphology (swelling and fragmentation) (5–8) to impaired activity of respiratory

chain complexes (9,10), weakened calcium buffering capacity (11) and mitochondria-dependent execution of apoptosis (12–14). Moreover, recent investigations have drawn attention to the presence of a generalized energetic imbalance both in patients and in mice, suggesting that ubiquitous defects in mitochondrial physiology might contribute to the disease process (15,16).

Compelling evidence has accumulated that uncontrolled association of mutSOD1 with mitochondria may be directly responsible for mitochondrial impairment (6,17,18), either by decreasing protein import selectively in spinal cord mitochondria (19) or by binding and inactivating specific mitochondrial targets such as the voltage-dependent anion channel 1 (20), the anti-apoptotic protein Bcl-2 (21) or the mitochondrial form of lysyl-tRNA synthetase (22). However, there is also indication that mitochondrial localization might not be necessary for mutant SOD1 (mutSOD1) to damage

*To whom correspondence should be addressed at: Laboratory of Neurochemistry, Fondazione S. Lucia Istituto di Ricovero e Cura a Carattere Scientifico, Via del Fosso di Fiorano 64, 00143 Rome, Italy. Tel: +39 06501703071; Fax: +39 06501703323; Email: m.cozzolino@hsantalucia.it

†M.T.C. and M.C. are Joint Senior Authors.

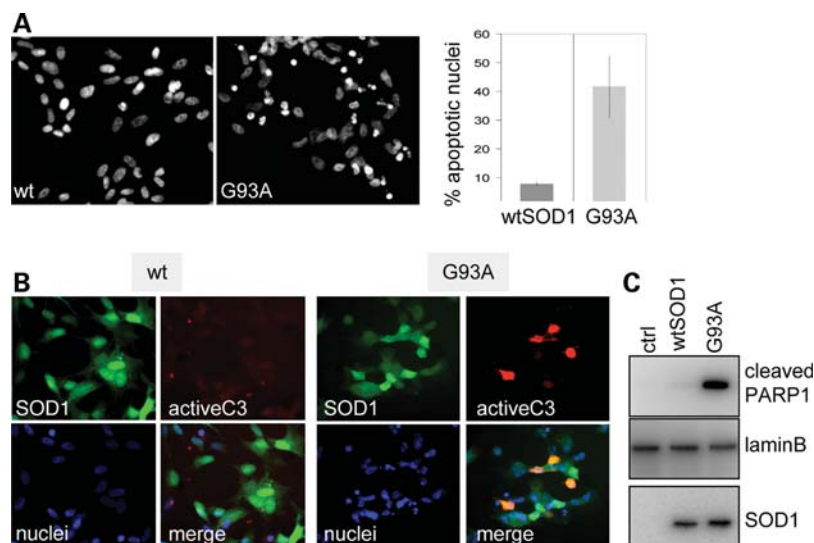


Figure 1. mutSOD1 induces apoptosis in SH-SY5Y cells. (A) SH-SY5Y cells were infected with adenoviruses coding for wild-type SOD1 (wtSOD1) or the fALS G93A-SOD1 mutant. After 72 h, nuclei of cells were stained with Hoechst 33342, and apoptotic nuclei were quantified as described in Materials and Methods. (B) Cells were infected as in (A) and analysed after 48 h by indirect immunofluorescence analysis with antibodies against SOD1 (green) or the active form of caspase-3 (activeC3, red). Cell nuclei are in blue. (C) After 72 h of expression of the indicated SOD1s, nuclear and cytosolic fractions from cells were isolated. Nuclei were analysed in western blot with antibodies recognizing the cleaved form of PARP1. The nuclear protein Lamin B was analysed as a standard for equal protein loading. Cytosolic fractions were also controlled for the expression of SOD1. Owing to the high levels of overexpressed exogenous mutSOD1s, endogenous mouse SOD1 in control cells is not evident in this exposure.

mitochondria (23), suggesting that cytosolic signals, yet to be identified, mediate the transfer of the inherent toxic properties of mutSOD1 to mitochondria.

A novel, mitochondria-related signalling mechanism involving the 66 kDa isoform of the growth factor adapter Shc (p66Shc), which is operative in conditions of oxidative stress, has been recently identified. The protein p66Shc is an alternatively spliced isoform of a growth factor adapter that is phosphorylated upon oxidative stress (24). In this form, a fraction of p66Shc localizes to mitochondria, where it binds to cytochrome *c* and acts as an oxidoreductase, generating ROS and leading to organelle dysfunction and cell death (25). p66Shc^{-/-} mice exhibit a 30% extended lifespan, reduced H₂O₂ levels and an enhanced resistance against oxidative stress (26), indicating that p66Shc acts as a key molecular sentinel that controls cellular stress responses and mammalian lifespan.

On the basis of these considerations, we have investigated the role of p66Shc in mutSOD1-induced cell toxicity, as well as the functional consequences of p66Shc ablation in transgenic mice overexpressing G93A-SOD1.

RESULTS

Apoptosis induced by mutSOD1 is accompanied by phosphorylation of p66Shc at serine 36

p66Shc is phosphorylated on a serine residue in position 36 in response to cellular stress induced by various stimuli, and this event is crucial to p66Shc-mediated oxidative stress and apoptosis (26,27). As an initial step to investigate the role of p66Shc in mutSOD1-induced cell stress, human wild-type or G93A-SOD1, the most studied SOD1 mutation associated

with familial amyotrophic lateral sclerosis (fALS), was transiently overexpressed in SH-SY5Y human neuroblastoma cells by adenoviral infection. In these conditions, G93A-SOD1 induces the sequential activation of caspase-3, cleavage of PARP and accumulation of fragmented nuclei, all suggestive of an ongoing apoptotic process (Fig. 1). Similar results were obtained when SH-SY5Y cells were infected with the fALS mutant H80R-SOD1 (Fig. 7 and not shown), indicating that the pro-apoptotic effect is common to fALS-linked SOD1s. In contrast, infection with adenoviruses expressing wtSOD1 or a control GFP protein (not shown) has no evident effects. To determine whether p66Shc is activated by mutSOD1 through phosphorylation on Ser36, total lysates from cells were immunoprecipitated with an anti-Shc antibody and analysed by western blotting using an antibody that specifically recognizes phosphorylated p66Shc at Ser36. Expression of G93A mutSOD1, but not of wtSOD1, induces p66Shc phosphorylation at Ser36 (Fig. 2A), whereas the expression levels of all Shc protein isoforms (p46, p52 and p66) are not affected.

Overexpression of dominant-negative, functionally inactive p66Shc proteins protects cells against mutSOD1-induced mitochondrial damage and apoptosis

To investigate the functional relevance of the phosphorylation of p66Shc at Ser36 induced by mutSOD1, SH-SY5Y cells stably overexpressing a serine 36-to-alanine (and therefore non-phosphorylatable) mutant of p66Shc (S36A; Fig. 2B) were infected with adenoviruses coding for wild-type SOD1 or G93A mutSOD1 and analysed after 72 h for apoptotic markers. As shown in Figure 2B, the number of apoptotic cells generated by mutSOD1 is reduced by ~90% in cells expressing the S36A mutant of p66Shc, and a similar decrease

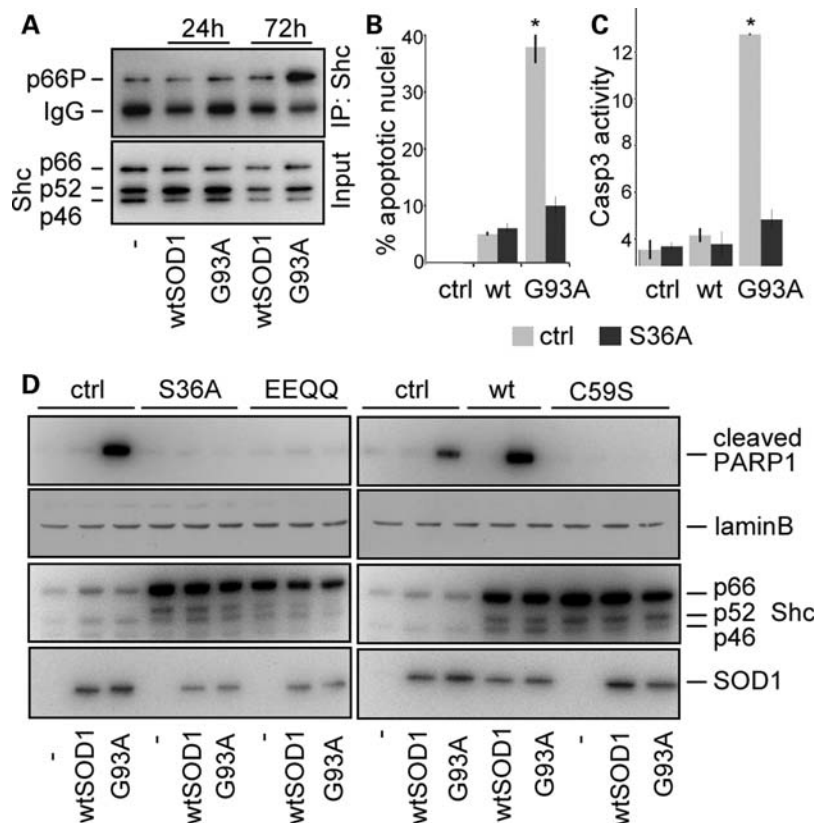


Figure 2. Functionally inactive mutant p66Shc protects cells from mutSOD1-induced apoptosis. (A) SH-SY5Y cells were infected with adenoviruses coding for wtSOD1 or the G93A mutSOD1. After the indicated times, cell lysates were subjected to immunoprecipitation with an anti-Shc antibody. Immunoprecipitates were analysed in western blot with an antibody recognizing p66Shc phosphorylated on serine 36 (p66P). The blot was re-probed with an anti-Shc antibody to check for equal protein input. (B) Control (ctrl) SH-SY5Y cells, or cells stably overexpressing the S36A non-phosphorylatable p66Shc mutant, were infected as in (A). After 72 h, cells were stained with Hoechst 33342 and apoptotic nuclei quantified. Values significantly different from relative controls are indicated with an asterisk when $P < 0.01$ ($n = 3$). (C) Cells treated as in (A) were assayed for the activity of caspase-3, expressed in arbitrary units. Two different clones of S36A p66Shc cells were analysed. Values significantly different from relative controls are indicated with an asterisk when $P < 0.01$ ($n = 3$). (D) Control SH-SY5Y cells, or cells stably overexpressing the S36A, C59S or E132Q/E133Q (EEQQ) mutants of p66Shc, were infected with adenoviruses coding for wtSOD1 or the G93A mutSOD1. After 72 h, nuclear and cytosolic fractions from cells were isolated. Nuclear fractions were analysed in western blot with antibodies anti-cleaved PARP1 and anti-lamin B, whereas cytosolic fractions were analysed with anti-SOD1 and anti-Shc.

in caspase-3 activity is observed (Fig. 2C). These data thus indicate that the phosphorylation of p66Shc plays a role in mutSOD1-induced cell death.

The pro-oxidant, pro-apoptotic activities of p66Shc depend upon two defined regions of the protein: two glutamic residues at position 132 and 133, the site where the redox activity of p66Shc has been mapped (25), and a cysteine at position 59, a regulatory disulphide/thiol site mediating a reversible dimer–tetramer transition, which has been proposed to control the protein’s apoptosis-inducing activity (28). When overexpressed in SH-SY5Y cells, both the E132Q/E133Q (EEQQ) and the C59S mutant p66Shc proteins are able to inhibit the pro-apoptotic activity of G93A mutSOD1, as measured by PARP cleavage, similar to what is observed with the S36A mutant (Fig. 2D). On the contrary, overexpression of wild-type p66Shc enhances the mutSOD1-induced apoptosis. Overall, these observations strongly indicate that p66Shc mediates the toxic effects exerted by mutSOD1.

It has been shown that mitochondrial Ca^{2+} responsiveness, which is a highly sensitive readout of mitochondrial state (27), is dramatically compromised after p66Shc activation.

Therefore, using the aequorin technology to monitor mitochondrial Ca^{2+} signalling (29), we analysed the effects of both wild-type and mutSOD1 proteins on SH-SY5Y cells displaying different background for p66Shc, i.e. in wild-type SH-SY5Y cells, in SH-SY5Y cells overexpressing the mutant S36A-p66Shc, in SH-SY5Y cells overexpressing the mutant EEQQ-p66Shc and in SH-SY5Y cells overexpressing wild-type p66Shc.

In SH-SY5Y cells, application of carbachol, an extracellular agonist acting on a Gq-coupled receptor, causes the production of inositol 1,4,5-trisphosphate and thus the release of Ca^{2+} from the endoplasmic reticulum and the transient increase of cytosolic and mitochondrial $[\text{Ca}^{2+}]$ (29).

In wild-type SH-SY5Y cells (Fig. 3A), the overexpression of wild-type SOD1 causes an increased mitochondrial $[\text{Ca}^{2+}]$ ($[\text{Ca}^{2+}]_{\text{m}}$) response after agonist stimulation. On the contrary, the overexpression of two different mutSOD1s causes a drastic reduction in the Ca^{2+} spike evoked by agonist stimulation, as an early consequence of mitochondrial damage as previously reported after p66Shc activation during oxidative stress (27).

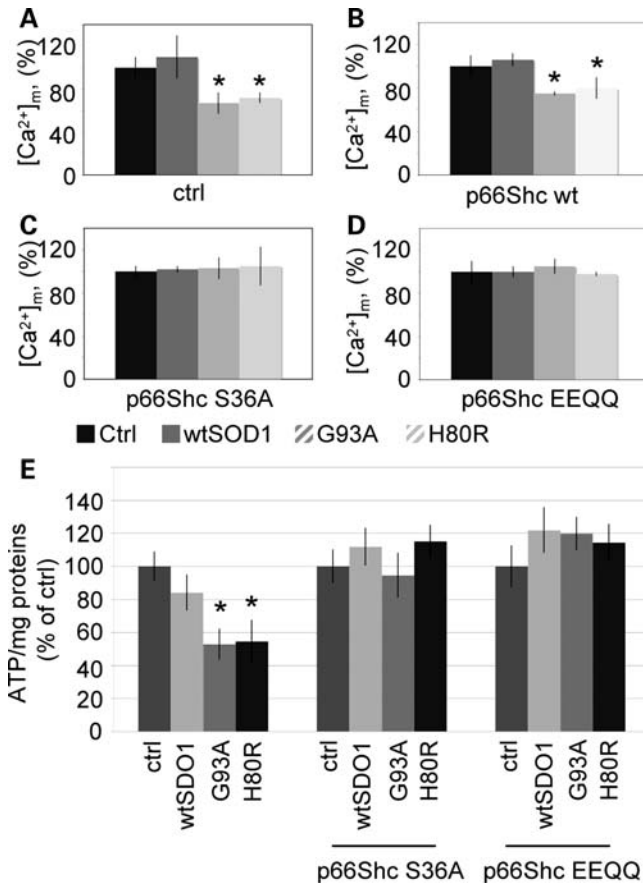


Figure 3. mutSOD1s cause mitochondrial damage in a p66Shc-dependent manner. Control SH-SY5Y cells (A), or cells stably overexpressing wild-type p66Shc (B), the S36A (C) or E132Q/E133Q (EEQQ, D) mutants of p66Shc, were infected with adenoviruses expressing wtSOD1 and the G93A or H80R mutSOD1s, together with an adenovirus expressing a mitochondrial targeted aequorin chimera. After 36 h, cells were challenged with 1 mM charbaol. The light signal was collected and calibrated into $[Ca^{2+}]_m$ values by an algorithm based on the Ca^{2+} response curve of aequorin at physiological conditions of pH, $[Mg^{2+}]$ and ionic strength. Statistical data are presented as mean \pm SEM. (E) SH-SY5Y cells, or cells stably overexpressing S36A or EEQQ mutant p66Shc, were infected with adenoviruses expressing wtSOD1 and the G93A or H80R mutSOD1s. After 48 h, total amount of ATP was assayed. The ATP concentration was normalized to total cellular protein concentration and expressed as percent of the relative, uninfected controls. Values are reported as mean \pm SD. Values significantly different from relative controls are indicated with an asterisk when $P < 0.05$ ($n = 3$).

The presence of p66Shc mutant proteins (Fig. 3C and D) confers mitochondrial insensitiveness to mutSOD1, since the mitochondrial Ca^{2+} response after agonist stimulation is almost unaffected by the presence of mutSOD1. On the contrary, the alteration of mitochondrial responsiveness induced by mutSOD1 is maintained in SH-SY5Y cells overexpressing wild-type p66Shc (Fig. 3B).

We have recently shown that mutSOD1 induces alterations in mitochondrial bioenergetics and morphology of SH-SY5Y cells (5). To test whether these effects arise as a consequence of p66Shc activation, ATP production and mitochondrial morphology were assayed in cells overexpressing wild-type or mutSOD1 together with p66Shc mutant proteins. To analyse the mitochondrial capability for energy production,

ATP concentration in SH-SY5Y cells exposed to mutSOD1s was measured. An [ATP] decrease was evident in cells overexpressing G93A or H80R mutSOD1 (Fig. 3E); in contrast, cells co-expressing functionally inactive p66Shc show a physiological ATP concentration.

As observed by immunofluorescence analysis of SH-SY5Y cells using antibodies anti-SOD1 and SOD2, a mitochondrial matrix protein (Fig. 4, left), cells expressing the G93A mutSOD1 show a significant alteration of the filamentous mitochondrial network which characterizes most of the untransfected or wild-type SOD1-transfected cells, with mitochondria appearing fragmented and swollen. Similarly, the filamentous network is essentially lost when cells are challenged with H_2O_2 . On the contrary, in cells expressing the p66Shc EEQQ mutant (Fig. 4, right), the overall filamentous network is maintained either in the presence of mutSOD1 or after H_2O_2 treatment. Similar results were obtained with the S36A mutant p66Shc (not shown).

On the whole, these data clearly indicate that p66Shc is the effector downstream of mutSOD1 responsible for the alterations of mitochondrial physiology that eventually lead to cell death.

Ablation of p66Shc significantly ameliorates ALS phenotype in mice

To learn whether transgenic G93A-SOD1 mice, an accepted model for ALS linked to mutSOD1, would be rescued by genetic removal of p66Shc, we crossed these mice with p66Shc $^{-/-}$ mice (26) and determined several behavioural and biochemical parameters.

As shown in Figure 5B, p66Shc is highly expressed in the spinal cord of control mice, as well as wtSOD1 or G93A-SOD1 transgenic mice, and only to a lower extent in the brain and muscle. As expected, ablation of p66Shc does not affect the levels of expression of transgenic SOD1 in the spinal cord. As shown in Figure 5A, G93A-SOD1/p66Shc $^{-/-}$ mice show significantly delayed onset of the disease (118.96 ± 10.98 versus 98.07 ± 8.9 days, $P < 0.0001$), improved motor performance as measured by rotarod test and increased survival (141.26 ± 14.42 versus 157.50 ± 9.11 days, $P < 0.0001$) with respect to G93A-SOD1 mice. Such striking effects are paralleled by improved mitochondrial function specifically in the spinal cord, where the activity of complex IV is restored (Fig. 5C) together with the ratio between reduced and oxidized glutathione (GSH/GSSG) in mitochondria, which is an indicator of the redox state of the cell (Fig. 5D).

p66Shc mediates the toxicity of mutSOD1 through Rac1 inactivation

To learn more on the molecular mechanisms of mutSOD1-induced p66Shc toxicity, and to attempt the dissection of such mechanisms *in vitro*, we focused on Rac1, a member of the Rho family of small GTPases, which controls many intracellular processes, including ROS production and cytoskeletal dynamics, and whose activity has been linked to the activity of both SOD1 and p66Shc (30,31).

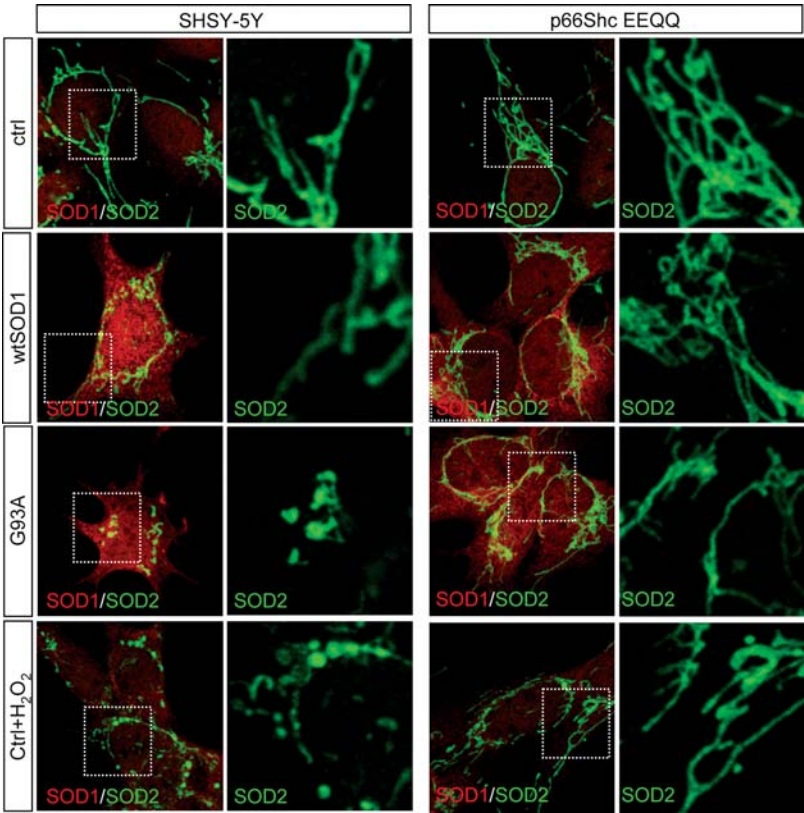


Figure 4. p66Shc inhibition prevents mitochondrial fragmentation induced by mutSOD1. SH-SY5Y control cells or p66Shc/EEQQ overexpressing cells were left untreated, or infected with adenoviruses coding for the indicated SOD1s. After 48 h, cells were subjected to immunofluorescence analysis with anti-SOD1 (green) and anti-SOD2 (red) antibodies. As a control for mitochondrial fragmentation, SH-SY5Y cells were treated with 500 μ M H₂O₂ for 30 min and processed for mitochondrial staining as above. Higher magnifications of areas highlighted in insets are shown.

Overexpression of both G93A and H80R mutant proteins decreases the levels of active, GTP-bound form of Rac1 in SH-SY5Y cells, compared with control and wtSOD1-expressing cells, as measured by a GST-PAK1 pull-down assay (Fig. 6A and B). The effect is specific for Rac1, since mutSOD1s do not significantly affect the activity of either RhoA or Cdc42, two small GTPases functionally related to Rac1 (Fig. 6A and B). Moreover, the overexpression by adenoviral infection of a constitutive active (V12) form of Rac1 completely protects SH-SY5Y cells from mutSOD1-induced apoptosis, whereas the expression of a dominant-negative, inactive (N17) mutant of Rac1 has no effect (Fig. 7). Significantly, N17 Rac1 is able to induce apoptosis in control cells, and to re-establish the apoptotic phenotype in cells where apoptosis induced by mutSOD1s overexpression has been hampered by co-expression of functional inactive mutants of p66Shc (Fig. 8A and B), suggesting that Rac1 acts downstream of p66Shc. More importantly, in cells expressing the dominant-negative mutant p66Shc-S36A, Rac1 is active even in the presence of mutSOD1s (Fig. 9A); on the contrary, when a wild-type p66Shc protein is overexpressed in cells, Rac1 activity is dramatically compromised by mutSOD1s (Fig. 9B). Altogether, these data thus clearly indicate that p66Shc activation is an obligatory step for mutSOD1 to inhibit Rac1, which in turn leads to cell death.

p66Shc downregulates Rac1 activity through a redox-dependent mechanism

It has been recently shown that the activity of Rac1 is physiologically controlled by the redox environment of the cell, according to a mechanism where SOD1 itself exerts a primary role (30). To test whether a redox-dependent mechanism could account for the inhibition of Rac1 activity following p66Shc activation, control SH-SY5Y cells or cells overexpressing a functional inactive mutant of p66Shc (S36A) were treated with H₂O₂ and the amount of GTP-Rac1 was assayed accordingly. Indeed, increasing concentration of H₂O₂ induces a proportional decrease in Rac1 activity, and this effect is associated with a strong decrease in cell viability (Fig. 10A and B). The expression of an S36A p66Shc mutant almost completely prevents H₂O₂-induced cell death, and in this condition the decrease in the activity of Rac1 is precluded (Fig. 10B and C). These results prompted us to investigate whether the activity of Rac1 could be affected by factors controlling the intracellular pool of GSH, which is the major determinant of the cellular redox state (32). As shown in Figure 10D, treatment of cells overexpressing mutSOD1 with the cell-permeable ethyl ester form of reduced GSH (GEE), which results in an increase in intracellular GSH, significantly restores Rac1 activity, whereas depletion of

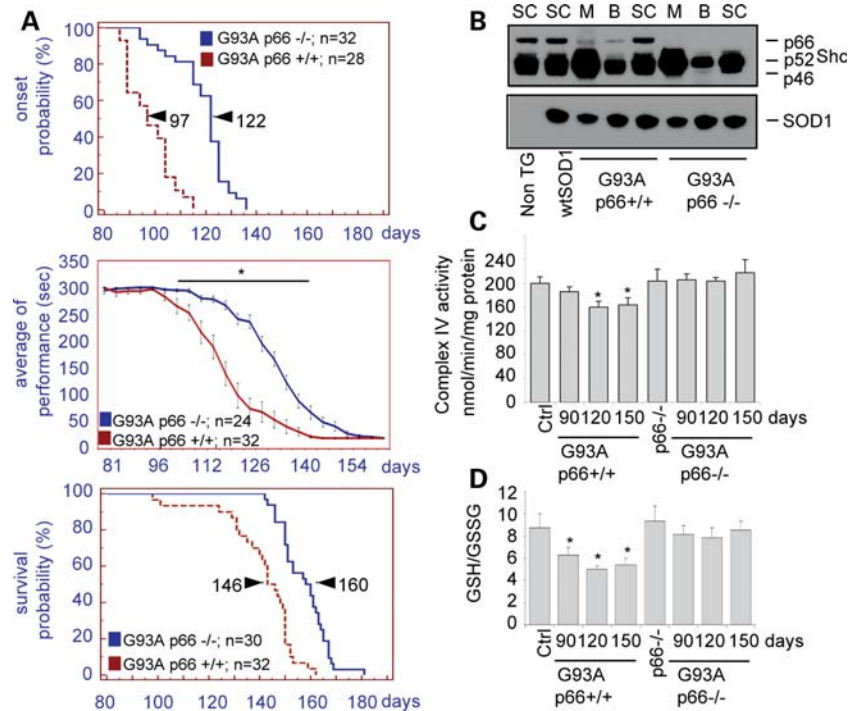


Figure 5. Downregulation of p66Shc ameliorates ALS phenotype in mice. (A) Transgenic mice overexpressing G93A-SOD1 were crossed with p66Shc^{-/-} mice and characterized for onset (grip test, top panel), motor performance (rotarod test, middle panel) and survival (bottom panel). Equal numbers of males and females were analysed for each genotype. No sex-dependence was observed and therefore data were pooled. Number of animals tested (*n*) and the median onset and survival probabilities (arrowheads) are shown. Values significantly different from relative controls are indicated with an asterisk when $P < 0.01$. (B) Western blot analysis of SOD1 and p66Shc in the brain (B), muscle (M) and spinal cord (Sc) from G93A-SOD1 and G93A-SOD1/p66Shc^{-/-} mice. As a control, p66Shc expression was analysed in non-transgenic mice and in mice overexpressing wild-type SOD1. (C) Complex IV activity were determined from mitochondria extracted from spinal cord of G93A-SOD1 and G93A-SOD1/p66Shc^{-/-} mice. Values are reported as mean \pm SD. Values significantly different from relative controls are indicated with an asterisk when $P < 0.05$ ($n = 3$). (D) HPLC determination of GSH/GSSG ratio in mitochondria extracted from spinal cord of G93A-SOD1 and G93A-SOD1/p66Shc^{-/-} mice. Values are reported as mean \pm SD. Values significantly different from relative controls are indicated with an asterisk when $P < 0.05$ ($n = 3$).

cytoplasmic GSH with L-buthionine-(S,R)-sulfoximine (BSO) has a striking inhibitory effect on the activity of Rac1.

DISCUSSION

In the present study, we show that inhibition of mitochondrial redox signalling by p66Shc is able to rescue viability in cell models and to improve survival in the mouse model for fALS linked to mutSOD1.

Indeed, it has been shown, both in models and patients, that the pathological phenotypes of ALS well correlate with alterations in all the processes related to or controlling mitochondrial function, i.e. morphology and bioenergetics, transportation and clearance, apoptosis and calcium buffering (33), thus sustaining a direct role of mitochondrial dysfunction in motor neuron degeneration in ALS pathogenesis.

However, evidence linking mitochondrial abnormalities to ALS is yet incomplete. Most of all, it is not entirely clear whether, and to what extent, mitochondrial preservation could be beneficial to the disease. To answer these questions, we decided to focus on p66Shc as a central regulator of mitochondrial ROS metabolism and the mitochondrial apoptosis pathway (24). p66Shc responds to a variety of stimuli by increasing ROS levels in the mitochondrial intermembrane space through an ROS-producing activity (25). The

physiological role of this process is currently unknown, although it is clear that it might participate in the control of intracellular redox-based signal transduction pathways (34). These mechanisms are indeed relevant for the process of apoptosis, since p66Shc-mediated formation of ROS triggers the initiation of the mitochondrial apoptosis pathway, and more generally for the regulation of lifespan (26) and energy metabolism (35,36), which are intimately connected. Moreover, p66Shc has a function in various pathological conditions where oxidative stress plays a role, such as arteriosclerosis (37) and endothelial dysfunctions (38).

Although it has been initially suggested that other, non-mitochondrial activities of p66Shc might be needed to exert its pro-apoptotic function (25), activation of the p66Shc pathway has emerged as a clear readout of mitochondrial damage in cells (39), and data presented in this work clearly point to the intrinsic, mitochondrial redox activity of p66Shc in mediating the toxicity exerted by mutSOD1. Different lines of evidence support this conclusion: (i) the accumulation in cells expressing mutSOD1 of p66Shc species phosphorylated on serine 36, a critical regulatory site for the mitochondrial pro-apoptotic activity of p66Shc (27), and the rescuing effect on cell viability of the non-phosphorylatable S36A p66Shc mutant; (ii) the inhibitory effect over the toxic action of mutSOD1s of the EEQQ and C59S p66Shcs, two

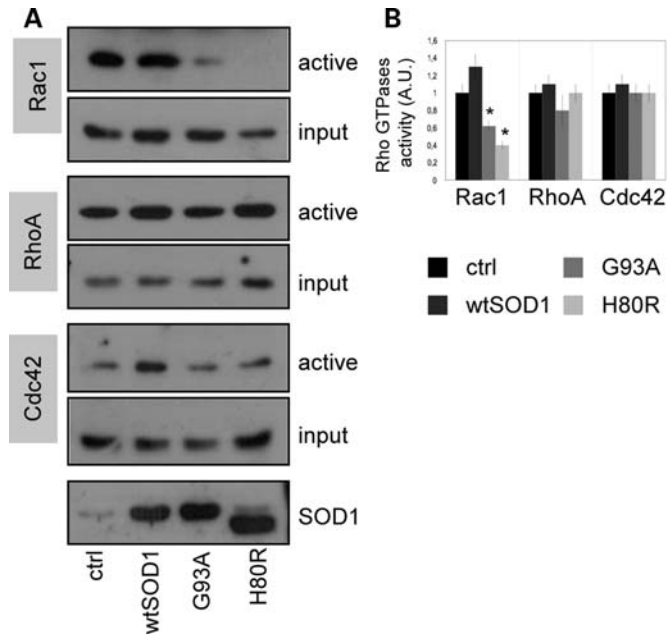


Figure 6. MutSOD1 proteins decrease Rac1-GTP levels in SH-SY5Y cells. (A) SH-SY5Y cells were infected with adenoviruses expressing wild-type or the G93A and H80R mutSOD1s. After 72 h, GTP-bound Rac1 and Cdc42 were pulled-down by a GST-PAK protein, whereas GTP-RhoA was pulled-down with a GST-Rothekin protein, both conjugated to GSH-sepharose. The GTP-bound (active) as well as the total (input) amounts of GTPases were detected in western blot using the indicated antibodies. Lysates were also analysed for SOD1 expression. (B) Quantification of active Rho GTPases in cells treated as in (A). The amounts of active GTPases were normalized to inputs and are expressed as mean \pm SD of arbitrary densitometric units relative to control, non-infected cells. Values significantly different from relative controls are indicated with an asterisk when $P < 0.01$ ($n = 4$).

mutants that are specifically endowed with mitochondrial redox activity (25,28); (iii) the recovery of mitochondrial function (as measured by rescued mitochondrial Ca^{2+} buffering capacity, ATP production and mitochondrial morphology) and of cell viability obtained by the expression of functionally inactive mutant p66Shc. On the whole, these data clearly support the notion that the p66Shc mitochondrial pathway is a key effector responsible for the alterations of mitochondrial physiology evoked by mutSOD1. This conclusion is further supported by our data *in vivo*, in transgenic mice overexpressing mutant G93A-SOD1 but lacking p66Shc, where onset, motor performance and survival are significantly improved, together with mitochondrial functionality, and is in agreement with recent findings showing that blocking the mitochondrial apoptotic pathway preserves motor neuron viability and function in a mouse model of ALS (40). Of note, although a striking effect of p66Shc removal is obtained on the disease onset in these mice, the outcome on the overall disease progression is relatively minor. This would indicate a central role of mitochondrial dysfunction in mediating disease initiation by mutSOD1, and of p66Shc as an important player participating in this process.

To clarify the molecular mechanisms by which p66Shc activation is responsible for neuronal cell damage induced by overexpression of mutSOD1s, we analysed the functional relationship between activation of p66Shc by mutSOD1 and

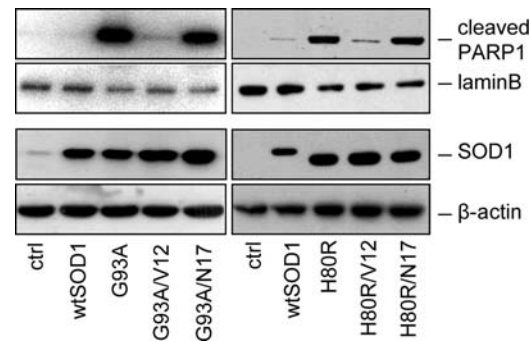


Figure 7. A constitutively active (V12) form of Rac1 completely protects SH-SY5Y cells from mutSOD1-induced apoptosis. SH-SY5Y cells were infected with adenoviruses expressing wild-type or the G93A (left panel) and H80R (right panel) mutSOD1s, in the absence or in the presence of adenoviruses coding for constitutive active (V12) or inactive (N17) mutants of Rac1. After 72 h, nuclear fractions from cells were isolated and analysed in western blot with antibodies anti-cleaved PARP1 and anti-lamin B. Cytosolic fractions were analysed with anti-SOD1, anti-Rac1 and anti-β-actin antibodies.

Rac1, a prominent member of Rho family of small GTPases. Rac1 is an intracellular transducer known to regulate multiple signalling pathways that control the organization of cytoskeleton, gene expression and cell proliferation (41). Rac1 and its relatives are also essential regulators of NADPH-dependent membrane oxidase (NOX) that produces superoxide anions, in both phagocytic and non-phagocytic cells (42), according to a mechanism where SOD1 itself seems to play a pivotal role. Indeed, Harraz *et al.* (30) have recently shown that when superoxide anions produced by microglial NOX exceed a physiological threshold, they are converted to hydrogen peroxide by SOD1, which normally binds to Rac1 itself and stimulates its activity. H_2O_2 then leads to the oxidative inactivation of Rac1, to the detachment of SOD1 from Rac1 and eventually to silencing of Rac1-dependent activity of NOX.

Similar to Harraz *et al.* (30), we also observed that Rac1 activity is strictly controlled, among other mechanisms, by redox conditions. However, we found that active Rac1 and cell viability are directly linked in neuronal cells, and that cell death induced by mutSOD1s is achieved through a p66Shc-dependent inhibition of Rac1, whereas it has been clearly shown that the pro-inflammatory activity of mutSOD1-expressing microglial cells relies on an uncontrolled, constitutive activation of Rac1 (30). Further, p66Shc was proposed to promote Rac1 activation (31), thereby triggering ROS production by NOX, whereas in our cell model, p66Shc activation is clearly responsible for Rac1 inhibition. The reasons for these apparent discrepancies can be partially explained by differences in the cellular milieu (neurons versus glia) and by the fact that the activity of Rho family GTPases is strictly dependent on their subcellular distribution and compartmentalization, which again can be profoundly different between neuronal and glial cells.

Nonetheless, different lines of evidence support a role of Rac1 inhibition in the process of neurodegeneration in ALS. Mutations in alsin, which are responsible for a recessive form of juvenile-onset ALS, are predicted to affect the guanine nucleotide exchange factor (GEF) activity of this

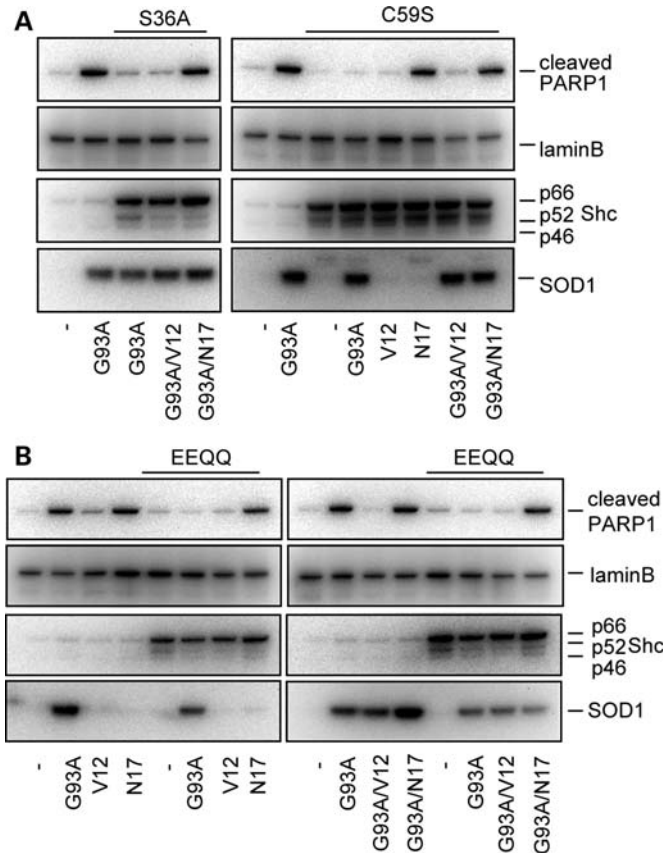


Figure 8. A constitutively inactive (N12) form of Rac1 re-establishes the apoptotic phenotype in cells overexpressing functional inactive mutants of p66Shc. Control SH-SY5Y cells, or SH-SY5Y cells expressing the S36A, C59S (A) or EEQQ (B) p66Shc mutants, were infected with adenoviruses coding for wild-type or the G93A and H80R mutSOD1s, in the absence or in the presence of adenoviruses expressing constitutive active (V12) or inactive (N17) mutants of Rac1. After 72 h, nuclear and cytosolic fractions from cells were isolated. Nuclear fractions were analysed in western blot with antibodies anti-cleaved PARP1 and anti-lamin B, cytosolic fractions with anti-Shc and anti-SOD1.

protein (43,44). Alsin knockdown inhibits axon growth and induces cell death in cultured motoneurons. Notably, these cellular phenotypes are mimicked by expression of a dominant-negative Rac1 mutant and are completely blocked by expression of a constitutively active Rac1 mutant (45). Overexpression of alsin protects NSC34 cells from mutSOD1-induced apoptosis, and this neuroprotective activity is completely inhibited by knocking down the endogenous Rac1 expression with siRNA for Rac1 (46). On the whole, these observations clearly point to disruption of Rac1 GTPase function as a causative event of motor neuron degeneration. This conclusion is further supported by recent results obtained in neuronal cells depleted of the 43 kDa TAR DNA-binding protein (TDP-43), a major component of the ubiquitinated inclusions characteristic of ALS and frontotemporal lobar degeneration with ubiquitin-positive inclusions, whose mutations have been causally linked to familial ALS. The knockdown of TDP-43 in differentiated Neuro-2a cells inhibits neurite outgrowth and induces cell death through the inactivation of Rho family members RhoA and Rac1, and

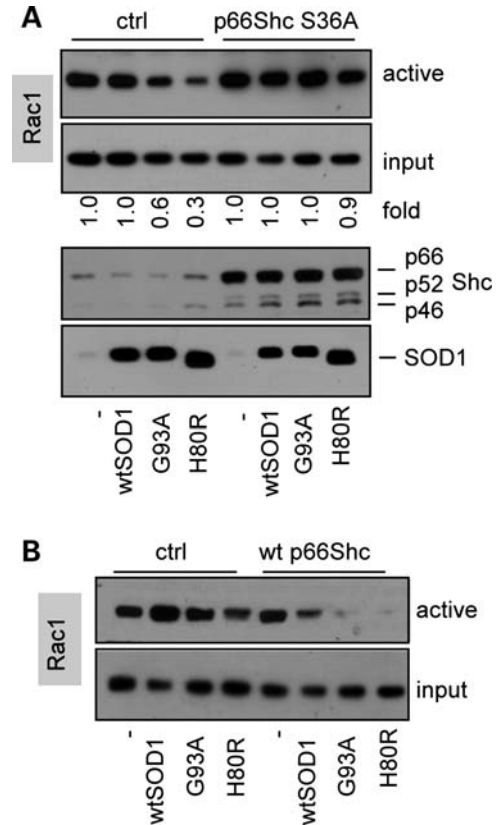


Figure 9. Inhibition of p66Shc prevents the downregulation of Rac1 activity induced by mutSOD1s. Control SH-SY5Y or SH-SY5Y cells expressing the S36A (A) or the wild-type (B) p66Shc proteins were infected with adenoviruses expressing wild-type SOD1 or the G93A and H80R mutSOD1s. After 72 h, GTP-bound Rac1 was analysed with a GST-PAK pull-down assay. The GTP-bound (active) as well as the total (input) amounts of Rac1 GTPase were detected in western blot using an anti-Rac1 antibody. Lysates were also analysed for p66Shc and SOD1 expression. The numbers represent fold activity above normalized activity in control uninfected cells (referred to as 1.0); densitometric scanning of the films was used to determine relative levels of Rac1 activation versus protein amounts. The data are representative of $n = 3$ independent experiments.

Cdc42 GTPases. These effects are associated with the inhibition of protein geranylgeranylation, a key post-translational modification for Rho family activity and intracellular localization (47). Our results point to a direct role of ROS in Rac1 inactivation, as suggested by the observation that the decrease of Rac1 activity by both hydrogen peroxide or mutSOD1 is prevented by inhibition of p66Shc-dependent mitochondrial redox signalling or by increased intracellular concentration of GSH. This is in line with recent findings indicating that GTPases may also be directly controlled by redox agents (48), a mechanism of regulation that may be particularly relevant in pathological conditions, such as ALS, where ROS are generated and the cellular redox balance altered.

In conclusion, our data emphasize that mitochondrial redox signalling, p66Shc and Rac1 are linked by an intimate connection in neurons *in vitro* and *in vivo*, in adult mice. That such connections are altered in a genetic context mimicking part of ALS patients strongly supports the concept that molecules involved in this signalling play an important role in this disease.

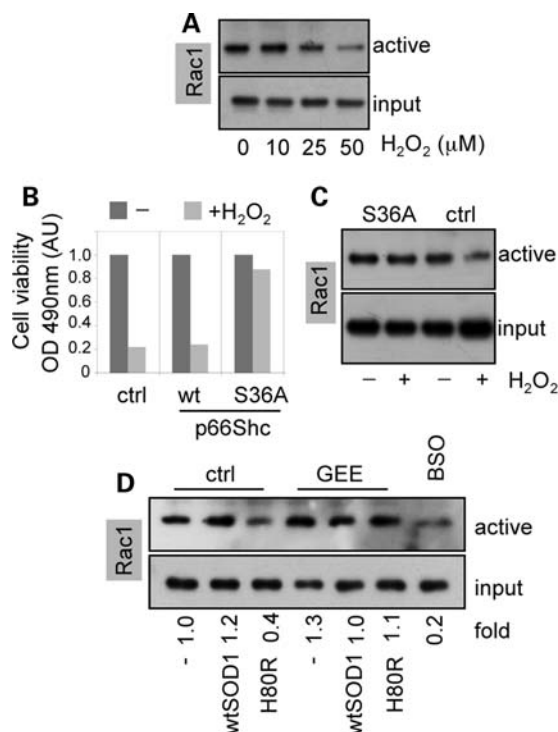


Figure 10. Redox regulation of Rac1 activity by mutSOD1. (A) SH-SY5Y cells were treated with the indicated amounts of H₂O₂. After 24 h, active Rac1 was measured by a GST-PAK pull-down assay. (B) The viability of control SH-SY5Y cells or SH-SY5Y cells expressing the S36A mutant p66Shc and treated with 50 μM H₂O₂ was calculated after 24 h through an MTS assay. (C) The activity of Rac1 was measured in cells treated as in (B). (D) SH-SY5Y cells were infected with adenoviruses expressing wtSOD1 or the H80R mutSOD1, in the absence or in the presence of 5 mM GEE. Control cells were also treated with 10 mM BSO. After 72 h, cell lysates were subjected to GST-PAK pull-down assay for the assessment of Rac1 activity. The numbers represent fold activity above normalized activity in control uninfected cells (referred to as 1.0). The data are representative of *n* = 3 independent experiments.

MATERIALS AND METHODS

Plasmid construction

Human cDNA coding for p66Shc (accession number U73377) was cloned by reverse transcription-PCR from human SH-SY5Y neuroblastoma cells cDNA, using the forward primer 5' AAA AAG CTT ATG GAT CTC CTG CCC CCC 3' and the reverse primer 5' TTT CTC GAG TCA CAG TTT CCG CTC CAC 3'. The resulting PCR fragment was inserted into *Hind*III/*Xho*I restriction sites of pcDNA3 (Invitrogen). For the mutagenesis of p66Shc, PCR site-directed mutagenesis was performed using pcDNA3/p66Shc as template, followed by digestion with *Dpn*I. All the plasmid constructions were verified by automated sequencing.

Cell culture, plasmid transfection and adenoviral infection

Human neuroblastoma cells, SH-SY5Y, were purchased from the European Collection of Cell Culture and grown in DMEM (Invitrogen) supplemented with 10% fetal calf serum (FCS, Euroclone), at 37°C in an atmosphere of 5% CO₂ in air. For stable expression of wild-type or mutant p66Shc, cells were

co-transfected with plasmids coding for different p66Shc proteins in the presence of 1:20 of a plasmid coding for hygromycin resistance, using Lipofectamine Plus reagent (Invitrogen). After selection with 400 mg/ml hygromycin (Invitrogen), about 20 clones for each construct were isolated independently and analysed in western blot with anti-Shc antibodies. At least three clones for each plasmid were chosen for equivalent expression of p66Shc proteins and used for further analysis. All the clones analysed gave consistent results and data from one clone are shown.

Construction of recombinant adenoviruses expressing wild-type SOD1, as well as G93A and H80R mutSOD1, was carried out by inserting cDNAs coding for the different SOD1s into the pShuttle2 and BD Adeno-X viral DNA (BD Bioscience). Transient transfections of HEK293 cells were performed using Lipofectamine 2000 (Invitrogen). Viral titre was determined by dilution assay using HEK293 cells according to the manufacturer's instructions. Adenoviruses were propagated in HEK293 cells as described in Latella *et al.* (49). Infection of SH-SY5Y cells was carried out for 1 h in OPTIMEM; after removal of the virus, cells were grown for the indicated period of times before being subjected to further experimental manipulations. To optimize the protocol for SH-SY5Y infection, cells were infected with Ad-GFP and Ad-SOD1s, and expression was measured by immunoblotting and immunofluorescence with the antibody anti-SOD1. Efficiency of infection was ~90% at a multiplicity of infection (m.o.i.) of 1000 after infection for 48 h. V12 and N17 Rac1 adenoviruses were described in Cozzolino *et al.* (50) and used at an m.o.i. of 50.

Nuclei isolation and cleaved PARP1 analysis

On 60 mm Petri dishes, 1.5×10^6 SH-SY5Y cells were plated. After the indicated treatments, cells were rinsed in ice-cold PBS and lysed in 150 μl of low-salt buffer (10 mM Hepes, pH 7.4, 42 mM KCl, 5 mM MgCl₂, 0.5 % CHAPS, 1 mM DTT, 1 mM PMSF, 1 mg/ml leupeptin). After centrifugation at 2000g, nuclei were resuspended in 50 μl of high-salt buffer (50 mM Tris-HCl, pH 7.5, 400 mM NaCl, 1 mM EDTA, 1% Triton X-100, 0.5% Nonidet-P40, 10% glycerol, 2 mM DTT, 1 mM PMSF, protease inhibitor cocktail). After 30 min on ice, lysates were centrifuged at 20 000g, supernatants were collected and analysed as nuclear fractions in western blot with antibodies anti-cleaved PARP1 (Cell Signalling) and anti-Lamin B (Santa Cruz Biotechnology).

Assessment of apoptosis and cell viability

Quantification of apoptotic cells was obtained by direct visual counting after nuclear staining of 4% paraformaldehyde-fixed cells with the fluorescent probe Hoechst 33342 (1 mg/ml) (Sigma-Aldrich). One hundred cells were examined for each field at a magnification of 200× and eight randomly chosen fields for each experimental condition were counted. Only the cells containing clearly picnotic or fragmented nuclei were considered apoptotic. Caspase 3 activity was measured with a TruePoint Caspase 3 assay kit (PerkinElmer), according to the manufacturer's instructions.

Cell viability was assessed by a colorimetric assay using the 3(4,5-dimethylthiazol-2-yl)-5-(3-carboxymethoxyphenyl)-2-(4-sulfophenyl)-2H-tetrazolium (MTS) assay (CellTiter 96 Aqueous One Solution Assay, Promega), according to the manufacturer's instructions. Absorbance at 490 nm was measured in a multilabel counter (Victor3-V, PerkinElmer Life Sciences).

Mitochondrial Ca^{2+} measurements

Cells were seeded before transfection onto 13 mm glass cover slips and allowed to grow to 50% confluence. At this stage, the cells were infected with the adenovirus expressing a mitochondrial targeted aequorin chimera. Thirty-six hours after infection, the cover slips with the cells were incubated with 5 mM coelenterazine for 1–2 h in DMEM supplemented with 1% FCS, and then transferred to the perfusion chamber. All aequorin measurements were carried out in KRB (Krebs–Ringer modified buffer: 125 mM NaCl, 5 mM KCl, 1 mM Na_3PO_4 , 1 mM MgSO_4 , 5.5 mM glucose, 20 mM HEPES, pH 7.4, 37°C) supplemented with 1 mM CaCl_2 . The agonist, 1 mM carbachol, was then added to the same medium. The experiments were terminated by lysing the cells with 100 μM digitonin in a hypotonic Ca^{2+} -rich solution (10 mM CaCl_2 in H_2O), thus discharging the remaining aequorin pool. The light signal was collected and calibrated into $[\text{Ca}^{2+}]$ values by an algorithm based on the Ca^{2+} response curve of aequorin at physiological conditions of pH, $[\text{Mg}^{2+}]$ and ionic strength, as previously described (29). Statistical data are presented as mean \pm SEM, significance was calculated by Student's *t*-test and correlation analysis was done with the SigmaPlot 5.0 software (SPSS, Inc.).

Immunofluorescence analysis

For immunofluorescence analysis, cells cultured on poly-L-lysine-coated glass cover slip were washed in PBS and fixed with 4% paraformaldehyde in PBS for 10 min. Fixed cells were washed in PBS followed by permeabilization with 0.1% Triton X-100 in PBS for 5 min. Cells were blocked for 1 h in 2% horse serum in PBS and incubated for 1 h at 37°C with primary antibodies: mouse monoclonal anti-active casp3 (Cell Signaling), rabbit anti-SOD1 (Stressgen), rabbit anti-SOD2 (Stressgen), mouse monoclonal anti-SOD1 (clone SD-G6, Sigma-Aldrich). Cells were washed in blocking buffer and incubated for 1 h with an Alexa Fluor 488 goat anti-mouse (Invitrogen) and Cy3 goat anti-rabbit (Jackson ImmunoResearch Laboratories) antibodies. After rinsing in PBS, cells were stained with 1 mg/ml Hoechst 33342 (Sigma-Aldrich) and examined under a Zeiss LSM 510 confocal microscopy. Fluorescence images were processed using Adobe Photoshop.

Measurement of cellular ATP

Measurement of cellular ATP was performed using the ATPlite Assay (Perkin Elmer-Cetus, Norwalk, CT, USA). In brief, cells seeded in 96-well microplates were resuspended in 50 μl of lysis buffer and mixed for 10 min. Forty microlitres of substrate solution (Luciferase/Luciferin) was added to each

sample. The luminescence was measured using a luminescence plate reader (Victor3-V, PerkinElmer Life Sciences). The ATP concentration was normalized to total cellular protein concentration estimated by Bradford protein assay (Bio-Rad).

Rho family pull-down assay

The Rac-GTP and Cdc42-GTP pull-down assay was performed as previously described (50). Briefly, cells were lysed in a buffer containing 50 mM Tris, pH 7.2, 100 mM NaCl, 5 mM MgCl_2 , 1 mM DTT, 10% glycerol, 1% Nonidet-P40, plus protease inhibitors. One-fiftieth of cell lysates were subjected to immunoblotting. Cell lysates were mixed with 10 mg of bacterially expressed GST-PAK (rat PAK amino acids 1–252) bound to GSH–sepharose and incubated at 4°C with tumbling for 30 min. Beads were collected by centrifugation and washed twice in lysis buffer before addition of Laemmli buffer and analysis by western blot with anti-Rac1 and anti-Cdc42 antibodies. For the RhoA-GTP pull-down assay, cell lysis and washes were done in 50 mM Tris–Cl, pH 7.2, 500 mM NaCl, 1% (v/v) Triton X-100, 5 mM MgCl_2 , 1 mM DTT and protease inhibitors. Bacterially expressed GST-Rhotekin (murine amino acids 7–89) bound to GSH–sepharose was used in place of PAK.

Immunoprecipitation

After rinsing the cultures with ice-cold PBS, cell lysis was performed in RIPA buffer (50 mM Tris–HCl, 0.5% Triton X-100, 0.25% Na-deoxycholate, 0.1% SDS, 150 mM NaCl, 1 mM EDTA, 5 mM MgCl_2) containing 1 mM PMSF and a protease inhibitor cocktail (Sigma-Aldrich). A clear supernatant was obtained by centrifugation of lysates at 17 000g for 10 min. Protein content was determined using Bradford protein assay (Bio-Rad). Equal amounts of lysates were incubated at 4°C for 2 h with a rabbit polyclonal anti-Shc antibody (Cell Signal) and the immunocomplexes were collected by binding to protein A-Agarose beads (Roche), followed by three washes with lysis buffer.

Electrophoresis and western blot

Standard SDS–PAGE was performed as described (10). Western blot was performed onto nitrocellulose membranes (Amersham), except for RhoA, Rac1 and Cdc-42 that were blotted onto PVDF membranes (Millipore). After incubation in Tris-buffered saline (TBS) solution containing 0.1% Tween 20 and 5% non-fat milk, filters were incubated for 2 h at room temperature with the indicated antibodies diluted in a 2% non-fat milk, 0.1% Tween 20/TBS solution. Immunoreactive SOD1 was detected with a rabbit polyclonal anti-SOD1 antibody (Stressgen). p66Shc proteins were detected using a mouse monoclonal anti-Shc antibody which recognizes all the three isoforms of Shc (p46, p52 and p66). Phosphorylated p66Shc on serine 36 was detected using a mouse monoclonal specific antibody (Alexis). A goat antibody (Santa Cruz Biotechnology) was used to detect the cleaved form of PARP1. Antibodies anti-RhoA and Cdc42 were from Santa Cruz Biotechnology. Anti-Rac1 was from

Millipore. β -Actin was detected using a mouse monoclonal antibody from Sigma. A goat antibody anti-Lamin B was from Santa Cruz Biotechnology.

Following extensive washing in 0.1% Tween 20/TBS solution, filters were incubated with the appropriated peroxidase-conjugated secondary antibodies, washed in 0.1% Tween 20/TBS solution and developed using the POD chemiluminescence detection system (Roche). Image analysis and quantifications were performed by Kodak Image Station (KDS IS440CF 1.1) with 1D Image Analysis software.

Animals

All animal procedures have been performed according to the European Guidelines for the use of animals in research (86/609/CEE) and the requirements of Italian laws (D.L. 116/92). The ethical procedure has been approved by the Animal Welfare Office, Department of Public Health and Veterinary, Nutrition and Food Safety, General Management of Animal Care and Veterinary Drugs of the Italian Ministry of Health.

At the indicated time, mice were anaesthetized with 500 mg/kg chloral hydrate, sacrificed and dissected for the different experiments. All efforts were made to minimize suffering. All animals have been raised and crossed in the indoor animal house in a 12 h light/dark cycle in a virus/antigen-free facility with controlled temperature and humidity and have been provided with water and food *ad libitum*.

Wild-type SOD1 mice B6.Cg-Tg(SOD1)²Gur/J and SOD1G93A mice B6.Cg-Tg(SOD1*G93A)¹Gur/J were purchased from The Jackson Laboratory and were on C57BL/6J background. p66Shc^{-/-} mice were also in the C57BL/6J background.

Mice compared in this study were all littermates and housed together to minimize environmental factors. Mice were genotyped using PCR protocols from The Jackson Laboratory.

Western blot analysis for p66Shc and SOD1 expression was carried out as described above on total protein extracts from various tissues obtained through homogenization in RIPA buffer.

Symptom onset, survival and rotarod analysis

Behavioural analysis was performed according to the standard operating procedures indicated by Ludolph *et al.* (51). Briefly, mice were considered terminally paralysed if they were unable to right themselves after 10 s of being placed on their side. To assess symptom onset, mice were subjected to grip test twice a week, starting at 70 days of age. Rotarod testing was performed using the accelerating rotarod apparatus (Ugo Basile 7650 model). The rod was accelerated at a constant rate of 4 r.p.m. starting from 3 r.p.m. for a maximum of 5 min. The time (seconds) at which the animal fell from the bar was recorded. Mice were tested twice a week for three trials, each starting at 80 days of age, until they were unable to remain on the rotarod for at least 20 s. The best trial per day was recorded and used for analysis. Each time point represents the mean \pm SE of performance of all mice at each data point as previously described (52).

Determination of complex IV activity and GSH/GSSG ratio were carried out on purified mitochondria as previously described (10).

Statistical analysis

Statistical analysis of rotarod data was performed using ANOVA. Kaplan–Meier curves were compared using the log-rank test. Comparisons of protein expression levels, complex IV activity and values of GSH/GSSG ratio were performed using two-tailed unpaired Student's *t*-test. *P*-values of <0.05 were considered significant.

ACKNOWLEDGEMENTS

We are grateful to Claudia Crosio and Ciro Iaccarino for helping with construction of adenoviruses, to Cristiana Valle and Simona Rossi for help with animal motor tests and to Silvia Middei for statistical analysis.

Conflict of Interest statement. None declared.

FUNDING

This work was supported by Association Francaise contre les Myopathies (Project 14354 to M.C.), by Fondation Thierry Latran and Neuron EraNet (to M.T.C.) and by the Italian Association for Cancer Research (AIRC), Telethon (GGP09128), the Italian Ministry of Education, University and Research (COFIN) and Italian Ministry of Health (to P.P.).

REFERENCES

1. Cozzolino, M., Ferri, A. and Carri, M.T. (2008) Amyotrophic lateral sclerosis: from current developments in the laboratory to clinical implications. *Antioxid. Redox Signal.*, **10**, 405–443.
2. Cassina, P., Cassina, A., Pehar, M., Castellanos, R., Gandelman, M., de Leon, A., Robinson, K.M., Mason, R.P., Beckman, J.S., Barbeito, L. *et al.* (2008) Mitochondrial dysfunction in SOD1G93A-bearing astrocytes promotes motor neuron degeneration: prevention by mitochondrial-targeted antioxidants. *J. Neurosci.*, **28**, 4115–4122.
3. Dobrowolny, G., Aucello, M., Rizzuto, E., Beccafico, S., Mammucari, C., Boncompagni, S., Belia, S., Wannen, F., Nicoletti, C., Del Prete, Z. *et al.* (2008) Skeletal muscle is a primary target of SOD1G93A-mediated toxicity. *Cell Metab.*, **8**, 425–436.
4. Dupuis, L., di Scala, F., Rene, F., de Tapia, M., Oudart, H., Pradat, P.F., Meininger, V. and Loeffler, J.P. (2003) Up-regulation of mitochondrial uncoupling protein 3 reveals an early muscular metabolic defect in amyotrophic lateral sclerosis. *FASEB J.*, **17**, 2091–2093.
5. Ferri, A., Fiorenzo, P., Nencini, M., Cozzolino, M., Pesaresi, M.G., Valle, C., Sepe, S., Moreno, S. and Carri, M.T. (2010) Glutaredoxin 2 prevents aggregation of mutant SOD1 in mitochondria and abolishes its toxicity. *Hum. Mol. Genet.*, **19**, 4529–4542.
6. Cozzolino, M., Pesaresi, M.G., Amori, I., Crosio, C., Ferri, A., Nencini, M. and Carri, M.T. (2009) Oligomerization of mutant SOD1 in mitochondria of motoneuronal cells drives mitochondrial damage and cell toxicity. *Antioxid. Redox Signal.*, **11**, 1547–1558.
7. Higgins, C.M., Jung, C. and Xu, Z. (2003) ALS-associated mutant SOD1G93A causes mitochondrial vacuolation by expansion of the intermembrane space and by involvement of SOD1 aggregation and peroxisomes. *BMC Neurosci.*, **4**, 16.
8. Kong, J. and Xu, Z. (1998) Massive mitochondrial degeneration in motor neurons triggers the onset of amyotrophic lateral sclerosis in mice expressing a mutant SOD1. *J. Neurosci.*, **18**, 3241–3250.

9. Mattiazzi, M., D'Aurelio, M., Gajewski, C.D., Martushova, K., Kiaei, M., Beal, M.F. and Manfredi, G. (2002) Mutated human SOD1 causes dysfunction of oxidative phosphorylation in mitochondria of transgenic mice. *J. Biol. Chem.*, **277**, 29626–29633.
10. Ferri, A., Cozzolino, M., Crosio, C., Nencini, M., Casciati, A., Gralla, E.B., Rotilio, G., Valentine, J.S. and Carri, M.T. (2006) Familial ALS-superoxide dismutases associate with mitochondria and shift their redox potentials. *Proc. Natl Acad. Sci. USA*, **103**, 13860–13865.
11. Jaiswal, M.K., Zech, W.D., Goos, M., Leutbecher, C., Ferri, A., Zippelius, A., Carri, M.T., Nau, R. and Keller, B.U. (2009) Impairment of mitochondrial calcium handling in a mtSOD1 cell culture model of motoneuron disease. *BMC Neurosci.*, **10**, 64.
12. Cozzolino, M., Ferri, A., Ferraro, E., Rotilio, G., Cecconi, F. and Carri, M.T. (2006) A β 1 mediates apoptosis and mitochondrial damage induced by mutant human SOD1s typical of familial amyotrophic lateral sclerosis. *Neurobiol. Dis.*, **21**, 69–79.
13. Guegan, C., Vila, M., Rosoklija, G., Hays, A.P. and Przedborski, S. (2001) Recruitment of the mitochondrial-dependent apoptotic pathway in amyotrophic lateral sclerosis. *J. Neurosci.*, **21**, 6569–6576.
14. Pasinelli, P., Houseweart, M.K., Brown, R.H. Jr and Cleveland, D.W. (2000) Caspase-1 and -3 are sequentially activated in motor neuron death in Cu,Zn superoxide dismutase-mediated familial amyotrophic lateral sclerosis. *Proc. Natl Acad. Sci. USA*, **97**, 13901–13906.
15. Dupuis, L., Oudart, H., Rene, F., Gonzalez de Aguilar, J.L. and Loeffler, J.P. (2004) Evidence for defective energy homeostasis in amyotrophic lateral sclerosis: benefit of a high-energy diet in a transgenic mouse model. *Proc. Natl Acad. Sci. USA*, **101**, 11159–11164.
16. Dupuis, L., Corcia, P., Fergani, A., Gonzalez De Aguilar, J.L., Bonnefont-Rousselot, D., Bittar, R., Seilhean, D., Hauw, J.J., Lacomblez, L., Loeffler, J.P. et al. (2008) Dyslipidemia is a protective factor in amyotrophic lateral sclerosis. *Neurology*, **70**, 1004–1009.
17. Magrane, J., Hervias, I., Henning, M.S., Damiano, M., Kawamata, H. and Manfredi, G. (2009) Mutant SOD1 in neuronal mitochondria causes toxicity and mitochondrial dynamics abnormalities. *Hum. Mol. Genet.*, **18**, 4552–4564.
18. Liu, J., Lillo, C., Jonsson, P.A., Vande Velde, C., Ward, C.M., Miller, T.M., Subramaniam, J.R., Rothstein, J.D., Marklund, S., Andersen, P.M. et al. (2004) Toxicity of familial ALS-linked SOD1 mutants from selective recruitment to spinal mitochondria. *Neuron*, **43**, 5–17.
19. Li, Q., Vande Velde, C., Israelson, A., Xie, J., Bailey, A.O., Dong, M.Q., Chun, S.J., Roy, T., Winer, L., Yates, J.R. et al. (2010) ALS-linked mutant superoxide dismutase 1 (SOD1) alters mitochondrial protein composition and decreases protein import. *Proc. Natl Acad. Sci. USA*, **107**, 21146–21151.
20. Israelson, A., Arbel, N., Da Cruz, S., Ilieva, H., Yamanaka, K., Shoshan-Barmatz, V. and Cleveland, D.W. (2010) Misfolded mutant SOD1 directly inhibits VDAC1 conductance in a mouse model of inherited ALS. *Neuron*, **67**, 575–587.
21. Pedrini, S., Sau, D., Guareschi, S., Bogush, M., Brown, R.H. Jr, Nanche, N., Kia, A., Trotti, D. and Pasinelli, P. (2010) ALS-linked mutant SOD1 damages mitochondria by promoting conformational changes in Bcl-2. *Hum. Mol. Genet.*, **19**, 2974–2986.
22. Kawamata, H., Magrane, J., Kunst, C., King, M.P. and Manfredi, G. (2008) Lysyl-tRNA synthetase is a target for mutant SOD1 toxicity in mitochondria. *J. Biol. Chem.*, **283**, 28321–28328.
23. Bergemalm, D., Jonsson, P.A., Graffino, K.S., Andersen, P.M., Brannstrom, T., Rehnmark, A. and Marklund, S.L. (2006) Overloading of stable and exclusion of unstable human superoxide dismutase-1 variants in mitochondria of murine amyotrophic lateral sclerosis models. *J. Neurosci.*, **26**, 4147–4154.
24. Gertz, M. and Steegborn, C. (2010) The lifespan-regulator p66Shc in mitochondria: redox enzyme or redox sensor? *Antioxid. Redox Signal.*, **13**, 1417–1428.
25. Giorgio, M., Migliaccio, E., Orsini, F., Paolucci, D., Moroni, M., Contursi, C., Pelliccia, G., Luzi, L., Minucci, S., Marcaccio, M. et al. (2005) Electron transfer between cytochrome *c* and p66Shc generates reactive oxygen species that trigger mitochondrial apoptosis. *Cell*, **122**, 221–233.
26. Migliaccio, E., Giorgio, M., Mele, S., Pelicci, G., Reboldi, P., Pandolfi, P.P., Lanfranccone, L. and Pelicci, P.G. (1999) The p66shc adaptor protein controls oxidative stress response and life span in mammals. *Nature*, **402**, 309–313.
27. Pinton, P., Rimessi, A., Marchi, S., Orsini, F., Migliaccio, E., Giorgio, M., Contursi, C., Minucci, S., Mantovani, F., Wieckowski, M.R. et al. (2007) Protein kinase C β and prolyl isomerase 1 regulate mitochondrial effects of the life-span determinant p66Shc. *Science*, **315**, 659–663.
28. Gertz, M., Fischer, F., Wolters, D. and Steegborn, C. (2008) Activation of the lifespan regulator p66Shc through reversible disulfide bond formation. *Proc. Natl Acad. Sci. USA*, **105**, 5705–5709.
29. Pinton, P., Rimessi, A., Romagnoli, A., Prandini, A. and Rizzuto, R. (2007) Biosensors for the detection of calcium and pH. *Methods Cell Biol.*, **80**, 297–325.
30. Harraz, M.M., Marden, J.J., Zhou, W., Zhang, Y., Williams, A., Sharov, V.S., Nelson, K., Luo, M., Paulson, H., Schoneich, C. et al. (2008) SOD1 mutations disrupt redox-sensitive Rac regulation of NADPH oxidase in a familial ALS model. *J. Clin. Invest.*, **118**, 659–670.
31. Khanday, F.A., Santhanam, L., Kasuno, K., Yamamori, T., Naqvi, A., Dericco, J., Bugayenko, A., Mattagajasingh, I., Disanza, A., Scita, G. et al. (2006) Sos-mediated activation of rac1 by p66shc. *J. Cell. Biol.*, **172**, 817–822.
32. Schafer, F.Q. and Buettner, G.R. (2001) Redox environment of the cell as viewed through the redox state of the glutathione disulfide/glutathione couple. *Free Radic. Biol. Med.*, **30**, 1191–1212.
33. Shi, P., Gal, J., Kwinter, D.M., Liu, X. and Zhu, H. (2010) Mitochondrial dysfunction in amyotrophic lateral sclerosis. *Biochim. Biophys. Acta*, **1802**, 45–51.
34. Giorgio, M., Trinei, M., Migliaccio, E. and Pelicci, P.G. (2007) Hydrogen peroxide: a metabolic by-product or a common mediator of ageing signals? *Nat. Rev. Mol. Cell. Biol.*, **8**, 722–728.
35. Berniakovich, I., Trinei, M., Stendardo, M., Migliaccio, E., Minucci, S., Bernardi, P., Pelicci, P.G. and Giorgio, M. (2008) p66Shc-generated oxidative signal promotes fat accumulation. *J. Biol. Chem.*, **283**, 34283–34293.
36. Tomilov, A.A., Ramsey, J.J., Hagopian, K., Giorgio, M., Kim, K.M., Lam, A., Migliaccio, E., Lloyd, K.C., Berniakovich, I., Prolla, T.A. et al. (2011) The Shc locus regulates insulin signaling and adiposity in mammals. *Aging Cell*, **10**, 55–65.
37. Napoli, C., Martin-Padura, I., de Nigris, F., Giorgio, M., Mansueto, G., Somma, P., Condorelli, M., Sica, G., De Rosa, G. and Pelicci, P. (2003) Deletion of the p66Shc longevity gene reduces systemic and tissue oxidative stress, vascular cell apoptosis, and early atherogenesis in mice fed a high-fat diet. *Proc. Natl Acad. Sci. USA*, **100**, 2112–2116.
38. Camici, G.G., Schiavoni, M., Francia, P., Bachschmid, M., Martin-Padura, I., Hersberger, M., Tanner, F.C., Pelicci, P., Volpe, M., Anversa, P. et al. (2007) Genetic deletion of p66(Shc) adaptor protein prevents hyperglycemia-induced endothelial dysfunction and oxidative stress. *Proc. Natl Acad. Sci. USA*, **104**, 5217–5222.
39. Pinton, P. and Rizzuto, R. (2008) p66Shc, oxidative stress and aging: importing a lifespan determinant into mitochondria. *Cell Cycle*, **7**, 304–308.
40. Reyes, N.A., Fisher, J.K., Austgen, K., VandenBerg, S., Huang, E.J. and Oakes, S.A. (2010) Blocking the mitochondrial apoptotic pathway preserves motor neuron viability and function in a mouse model of amyotrophic lateral sclerosis. *J. Clin. Invest.*, **120**, 3673–3679.
41. Etienne-Manneville, S. and Hall, A. (2002) Rho GTPases in cell biology. *Nature*, **420**, 629–635.
42. Werner, E. (2004) GTPases and reactive oxygen species: switches for killing and signaling. *J. Cell Sci.*, **117**, 143–153.
43. Topp, J.D., Gray, N.W., Gerard, R.D. and Horazdovsky, B.F. (2004) Alsln is a Rab5 and Rac1 guanine nucleotide exchange factor. *J. Biol. Chem.*, **279**, 24612–24623.
44. Yang, Y., Hentati, A., Deng, H.X., Dabbagh, O., Sasaki, T., Hirano, M., Hung, W.Y., Ouahchi, K., Yan, J., Azim, A.C. et al. (2001) The gene encoding alsln, a protein with three guanine-nucleotide exchange factor domains, is mutated in a form of recessive amyotrophic lateral sclerosis. *Nat. Genet.*, **29**, 160–165.
45. Jacquier, A., Buhler, E., Schafer, M.K., Bohl, D., Blanchard, S., Beclin, C. and Haase, G. (2006) Alsln/Rac1 signaling controls survival and growth of spinal motoneurons. *Ann. Neurol.*, **60**, 105–117.
46. Kanekura, K., Hashimoto, Y., Kita, Y., Sasabe, J., Aiso, S., Nishimoto, I. and Matsuoka, M. (2005) A Rac1/phosphatidylinositol 3-kinase/Akt3 anti-apoptotic pathway, triggered by AlslnLF, the product of the ALS2 gene, antagonizes Cu/Zn-superoxide dismutase (SOD1) mutant-induced motoneuronal cell death. *J. Biol. Chem.*, **280**, 4532–4543.

47. Iguchi, Y., Katsuno, M., Niwa, J., Yamada, S., Sone, J., Waza, M., Adachi, H., Tanaka, F., Nagata, K., Arimura, N. *et al.* (2009) TDP-43 depletion induces neuronal cell damage through dysregulation of Rho family GTPases. *J. Biol. Chem.*, **284**, 22059–22066.
48. Aghajanian, A., Wittchen, E.S., Campbell, S.L. and Burridge, K. (2009) Direct activation of RhoA by reactive oxygen species requires a redox-sensitive motif. *PLoS One*, **4**, e8045.
49. Latella, L., Sacco, A., Pajalunga, D., Tiainen, M., Macera, D., D'Angelo, M., Felici, A., Sacchi, A. and Crescenzi, M. (2001) Reconstitution of cyclin D1-associated kinase activity drives terminally differentiated cells into the cell cycle. *Mol. Cell. Biol.*, **21**, 5631–5643.
50. Cozzolino, M., Stagni, V., Spinardi, L., Campioni, N., Fiorentini, C., Salvati, E., Alema, S. and Salvatore, A.M. (2003) p120 Catenin is required for growth factor-dependent cell motility and scattering in epithelial cells. *Mol. Biol. Cell.*, **14**, 1964–1977.
51. Ludolph, A.C., Bendotti, C., Blaugrund, E., Chio, A., Greensmith, L., Loeffler, J.P., Mead, R., Niessen, H.G., Petri, S., Pradat, P.F. *et al.* (2010) Guidelines for preclinical animal research in ALS/MND: a consensus meeting. *Amyotroph. Lateral Scler.*, **11**, 38–45.
52. Pizzasegola, C., Caron, I., Daleno, C., Ronchi, A., Minoia, C., Carri, M.T. and Bendotti, C. (2009) Treatment with lithium carbonate does not improve disease progression in two different strains of SOD1 mutant mice. *Amyotroph. Lateral Scler.*, **10**, 221–228.